

Empirical Characterization of Non-Intentional Emissions generated by PV Installations

G. Txertudi, U. Txertudi, M. Fernández, A. Gallarreta, J. González-Ramos and D. de la Vega

Bilbao Engineering College,
University of the Basque Country (UPV/EHU)
48013 Bilbao, Bizkaia, Spain;
Phone number: +34 946014133

Abstract. Non-Intentional Emissions (NIEs) generated by solar photovoltaic (PV) systems have significantly increased concerns about disturbances in the 9-150 kHz band of the low-voltage distribution grid, which can lead to failures or cause thermal stress in the devices connected to the grid. Moreover, these emissions can cause interference in narrowband power line communications (NB-PLCs). This paper presents a characterization of emissions generated by different real PV systems. Specifically, measurement campaigns were carried out in isolated PV systems, which employed different panel configurations, as well as in a grid-connected system. The analysis of the NIEs allows the identification of the frequencies and amplitudes of the emissions, as well as the evaluation of the NIEs variation over time. In addition, the impedances of the PV systems were also measured to correlate impedance variations with emissions.

Key words. Power line communications, photovoltaic installations, non-intentional emissions, impedance measurements.

1. Introduction

Photovoltaic (PV) solar energy is very promising because of its sustainability and environmental friendliness, but it is not free of challenges, especially with regard to its impact on the power grid. One of the major drawbacks of these systems involves the generation of conducted non-intentional emissions (NIEs) in the 9-150 kHz range that propagate through the low-voltage (LV) distribution grid [1]. These conducted emissions appear as unwanted energy in the form of electrical disturbances, which can have a range of adverse effects, such as interference with sensitive electronic devices, disruptions in the quality of electrical energy, and even impairments in communication through the electricity grid [2,3]. Moreover, these inconveniences can inflict harm on the equipment connected to the grid by subjecting them to thermal stress and causing damage, ultimately compromising overall system efficiency [2,4-6].

Ongoing efforts are being carried out to characterize these conducted emissions in both frequency and time domains to ensure a suitable power quality and to evaluate their impact on Power Line Communications (PLC) [7]. Several works were carried out to analyze the conducted emissions in the power grid. In [8,9] conducted emissions from different PV inverters in laboratory environments were

analyzed, but the network conditions were fixed. To ensure real LV grid conditions conducted emissions were also recorded in real installations [10]. However, to characterize properly conducted emissions from real PV systems, it is necessary to continue performing measurements in different real situations, which consider various configurations of the PV systems. Moreover, the influence of the system impedance should be also taken into account to better understand the propagation of conducted emissions into the grid.

A. Objective

This work presents an evaluation of NIEs generated by different real PV installations between 9-150 kHz range. Several measurement campaigns were carried out in isolated, and grid connected systems. Furthermore, system impedance was also taken into account.

2. Methodology

A. Measurement Scenarios

In this study, measurement campaigns were conducted on PV installations located at the University of the Basque Country (UPV/EHU) (Eibar section). Specifically, these installations are situated within the PV Laboratory, which is located on the third floor, and includes different types of PV systems connected to various types of solar panels. These solar panels are located on an outdoor terrace next to the laboratory.

Both standalone and grid-connected installations were chosen for investigation and various panel interconnections, both in parallel and in series, were examined. To ensure the robustness and reliability of the results, measurements were taken over several days with different weather conditions. Furthermore, impedance measurements were conducted to correlate variations of conducted emissions with changes in system impedance.

1) Off-grid systems

The measurement scenarios for off-grid systems include an installation that has the panels connected in series and another with the panels connected in parallel.

1.1) Installation 1: panels connected in series

The first configuration represents an isolated system characterized by utilizing two 80-Watt peak (80-W_p) monocrystalline PV panels connected in series. In this setup, the generated current flows from the connection box to a maximum power point tracking (MPPT) load regulator, capable of supporting 34 V. The primary function of this regulator is to manage the battery charge effectively while operating the systems at their maximum protection and power point. As shown in Fig. 1, there are two distinct pathways for supplying the required intensity. When sunlight is available, the current flows directly from the regulator to the inverter. Conversely, in overcast conditions, the system draws power from the battery. The inverter responsible for converting the generated direct current (DC) into alternating current (AC) is the TBS PS600-12 model, manufactured by TBS Electronics, and the energy storage component utilized is the Classic battery OPzS Solar 140 12V TV. The system incorporates magnetothermal and differential switches.

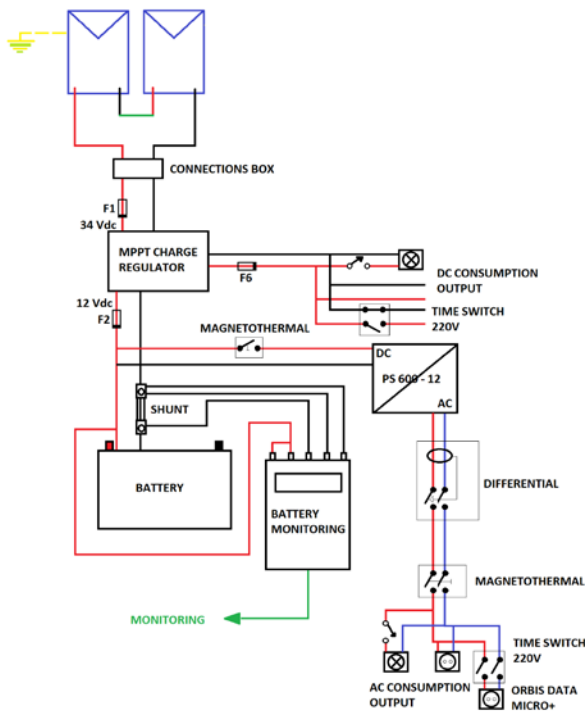


Fig.1. Installation 1 diagram

1.2) Installation 2: panels connected in parallel

The core components and devices of this isolated system are those of the first installation, including PV panels, the MPPT load regulator, the battery, the inverter, and protective switches. The only difference from the first installation lies in the panel arrangement, which now employs parallel connections. In this case, the MPPT has to handle 17 Vdc instead of 34 Vdc, as well as double intensity compared to installation 1.

2) Grid connected system

The PV installation connected to the grid consists of two monocrystalline panels, PV-JKM-175M model from Jinko Solar, each with a power of 175 W_p, resulting in a total system power of 350 W_p. The panels are connected to the

circuit breaker and the inverter, which is the Mastervolt SOLADIN 600 and is also connected to a screen for monitoring purposes. Once a sinusoidal waveform is created, after passing through the protections of the magnetic circuit breakers (10 A) and the differential circuit breaker (30 mA/40 A), the bidirectional meter is located, which operates at 220 V and 50 Hz, and after it the current flows to the connection box of the room. It is worth noting that the energy obtained from this setup is used to power the lights and devices of the PV laboratory. Additionally, any excess energy is delivered to the grid.

Since this system is connected to the grid, the recordings were performed with the inverter switched on and off to evaluate the effect of the installation on the grid.

B. Methodology for characterizing NIEs

1) Acquisition system

A voltage probe was connected to the plug to measure the conducted emission levels of the installations. The probe was presented in [11] and consists of a band-pass filter ranging from 9 to 500 kHz. It provides galvanic isolation and protection to the measurement equipment. The probe was connected to a digital oscilloscope (Picoscope Series 5000) that records and samples the received conducted emissions. The latter instrument has a 16-bit resolution and a sampling frequency of 8.92 MS/s. A laptop was connected to the oscilloscope via USB to control and monitor the equipment, as well as to store the measured data.

Finally, a portable generator was used to power the oscilloscope and the laptop to avoid conducted emissions due to the measurement equipment.

2) Assessment method

Two methods were employed for processing the acquired raw data and obtaining NIE. Firstly, the CISPR-16 [12], which provides QP values and is therefore suitable for comparison with conducted emission limits. This method employs a Lanczos window with a temporal resolution of 2 ms, achieved through its time overlap, and has a frequency-step-size of 50 Hz, resulting in a resolution bandwidth of 200 Hz.

Secondly, the IEC 61000-4-7 [13] method was used, which provides RMS values and a temporal resolution of 200 ms, achieved using rectangular windows without any overlap. The resolution bandwidth of this method is equal to 200 Hz.

For each setup and situation, one-minute measurements were taken. Moreover, these samples were analyzed every 3 seconds to get the outcome. Results were presented in the joint time-frequency and frequency domains, using spectrograms and traces, respectively. The latter show the emission level obtained for the 3-second data set.

C. Methodology for measuring system impedance

The access impedance of the electrical grid is highly variable and depends on factors such as the number and type of connected loads [14]. Since the tests have been carried out on different PV systems while connecting several loads, the impedance was also measured for the different situations. The impedance measurement method was developed by TSR Group at UPV/EHU [14]. As shown in Fig. 2, the method is based on measuring both voltage and current generated by a test signal injected into the electrical grid. As a result, the grid impedance is obtained. The laptop configures the test signals, automates the measurements, and stores the recordings for subsequent data processing.

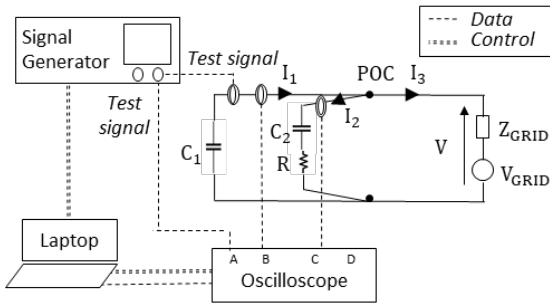


Fig.2. Impedance measurement method [14]

3. Result and analysis

A. Off-grid systems

To ensure that the inverter was working, a device that consumes power must be plugged into the installation, so a screen and a lamp were connected as loads. Figs. 3 and 4 show the emissions generated by the two isolated installations, processed using the CISPR-16 method. As shown, when connecting the loads, there are more narrowband emissions, especially in the 25-75 kHz frequency range. This is caused not only by the PV system emissions but also because of the NIEs introduced by the connected device. These events that occur when the load is connected make it challenging to distinguish the inverter's response. An interesting finding is that when the screen is connected high-frequency emissions (i.e. frequencies higher than 100 kHz) are attenuated.

The reduction of emissions amplitude can be attributed to the shift in system impedance when the device is plugged in. This can be observed in Fig. 5, where the system impedance is provided for the two isolated installations when no load is connected and where the screen or the light is connected to the system. As shown, the variation of the impedance magnitude with frequency is evident, and the highest impedance value is reached when no load is connected. When the light is plugged in, there is a slight reduction in the impedance value in both installations, and when the screen is connected the system impedance decreases significantly. In addition, in the latter case, the frequency at which the impedance reaches its maximum level also varies.

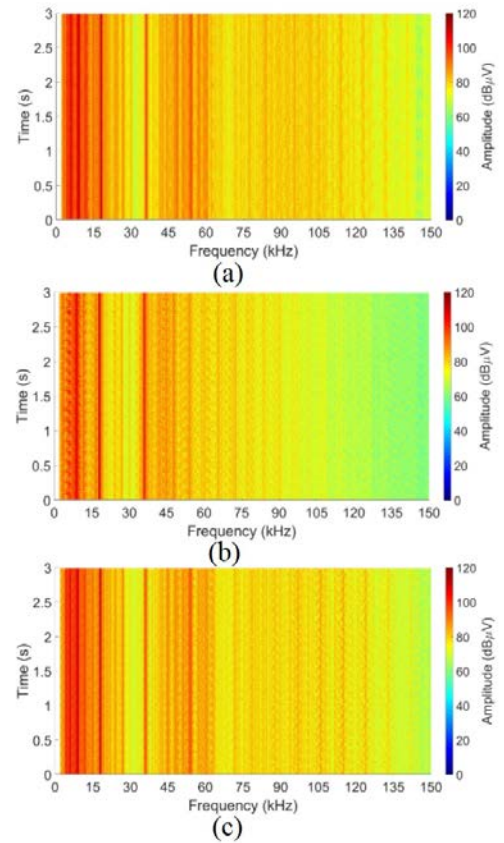


Fig.3. Spectrograms of NIEs processed with CISPR 16 and measured in installations with panels in parallel; (a) without load, (b) with the screen and (c) with the lamp.

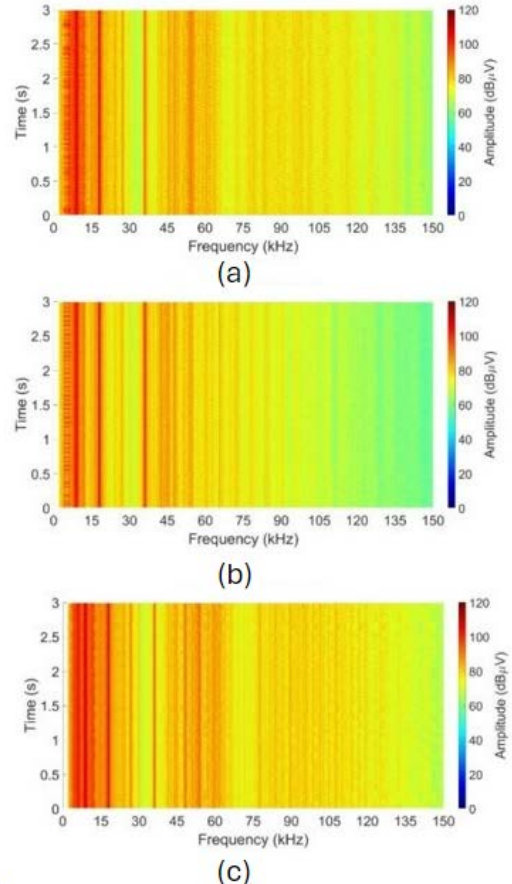


Fig.4. Spectrograms of the conducted emissions processed with CISPR 16 and measured in installations with panels in series; (a) without load, (b) with the screen and (c) with the lamp.

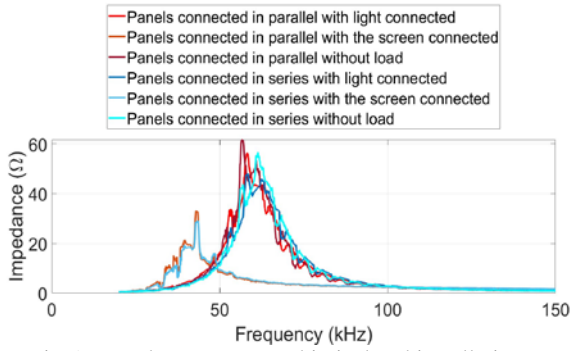


Fig.5. Impedances measured in isolated installations.

NIEs recorded in these two isolated installations are also presented in Fig. 6, where the IEC 61000-4-7 method was employed to compare the obtained results when no load is connected. As observed, the amplitude of the emissions is very similar in both cases, except at higher frequencies, where the installation with the panels in parallel presents higher values than the installation with the panels connected in series.

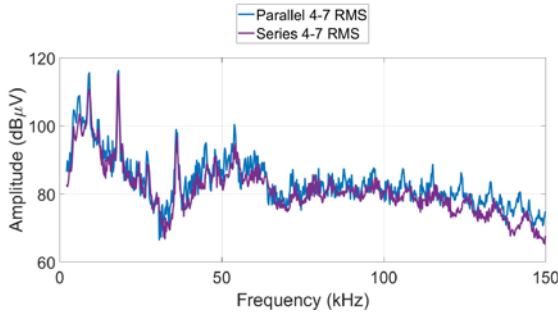


Fig.6. NIEs at isolated installations processed using the IEC 61000-4-7 method.

The impedance changes across frequencies were analysed, but no differences between higher and lower frequencies were found, so the slight variations in emissions amplitude observed in Fig. 6 were not attributed to impedance variations. However, to better understand the variations in emissions between the two installations found in Fig. 6, the spectrograms of NIEs for the different frequency ranges are presented in Figs 7 and 8. At lower frequencies, the temporal evolution of emissions was similar for both installations (i.e. the installation with the panels connected in series and the installation with the panels in parallel), as can be observed from Fig. 7. However, at higher frequencies, temporal variations are different in each installation. As shown in Fig. 8, the emissions generated by the installation with the panels in series not only have a lower amplitude around 120 kHz, but also do not follow the same temporal trend as at other frequencies. However, the installation with the panels in parallel does not present that difference in the temporal trend of emissions.

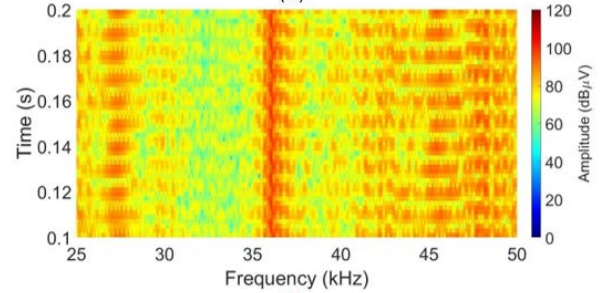
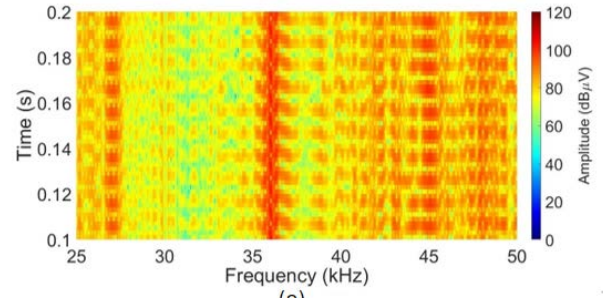


Fig.7. Variation over time of NIEs measured in installation with a) panels in series and installation with b) panels in parallel at low frequencies processed with the CISPR-16 method.

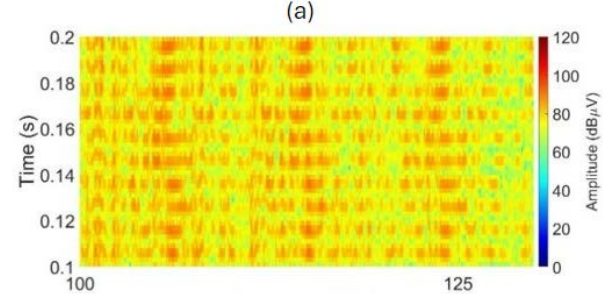
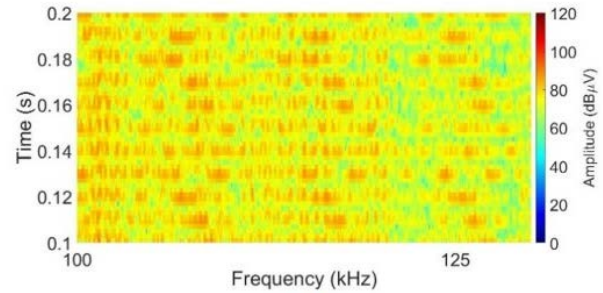


Fig.8. Variation over time of NIEs of installation with (a) panels in series and installation with (b) panels in parallel at high frequencies with the CISPR-16 method with out load.

For a more detailed analysis, the impedance variations over time are provided in Fig. 9. As shown, the impedance variations within 20 ms (corresponding to one cycle the AC signal) is very similar in both cases. Thus, differences in the variation of emissions between the two installations are not related to impedance variations.

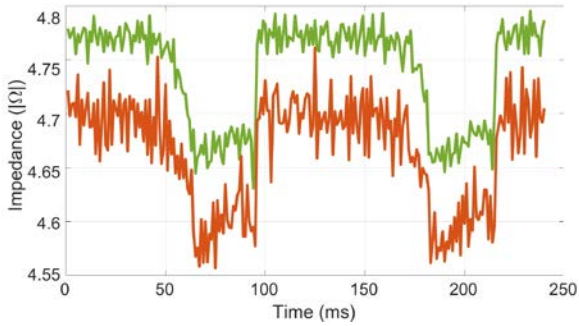


Fig.9. Sub-cycle impedance change within 20 ms in installations 1 and 2

Regarding the NIEs over frequency of both installations presented in Fig. 6, emissions appear at frequencies multiples of 6 and 9 kHz, implying that the switching frequencies of both the regulator and the inverter are these. At frequencies above 75 kHz, these harmonics of 6 and 9 kHz are no longer detected since, due to signal attenuation, emissions amplitude may be masked by background noise.

B. Grid connected system

The spectrograms obtained according to the CISPR-16 method of the measurements taken both with and without the inverter working are depicted in Fig. 10. As can be observed when the inverter is working, two narrowband emissions appear at 25 and 48 kHz, which are not present in the grid when the inverter is disconnected. Emissions at other frequencies are not related to the PV system, but to the grid, as they also appeared when the installation was switched off. No emissions at other frequencies due to the installation were found, but they may be masked by grid background noise and emissions.

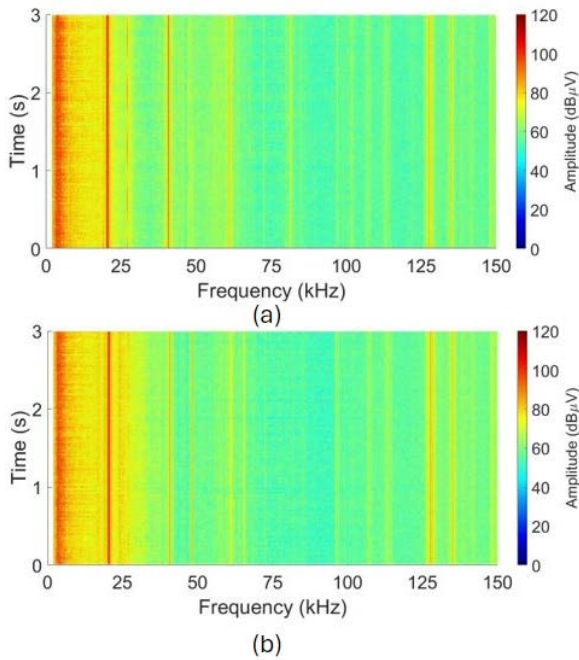


Fig.10. Spectrograms using the CISPR 16 method (a) with the inverter switched on, (b) with the inverter switched off

Another interesting phenomenon occurs at 28 kHz, since a narrowband emission appears in some measurements but only when the inverter is disconnected (i.e. when

emissions from the grid but not from the PV system are recorded). This can be caused by a device connected to the LV grid, but as can be observed in Fig. 11, when the inverter is connected the impedance at 28 kHz is almost zero, attenuating in this way NIEs at that frequency.

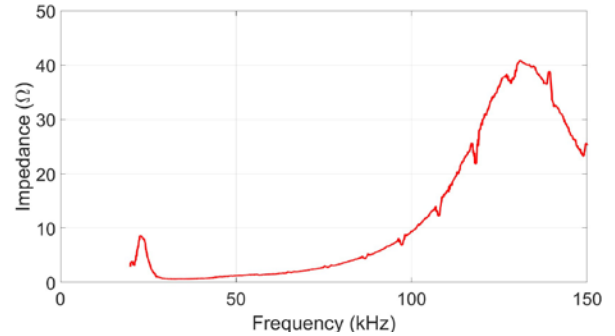


Fig.11. Impedance measured on the grid connected system

The traces of the measurements performed in the grid connected system and processed employing the IEC 61000-4-7 method are presented in Fig. 12. As shown, the narrowband emission at 48 kHz can be clearly distinguished when the inverter is operating, but it disappears completely when the inverter is switched off. The emission at 25 kHz can also be observed, although its amplitude is lower, as shown in the spectrogram of Fig. 10. Finally, the previously detected narrowband emission at 28 kHz (emission from the grid but not from the PV system) that disappears when the inverter works due to the impedance drop at that frequency is also observed in the results processed using the IEC 61000-4-7 method.

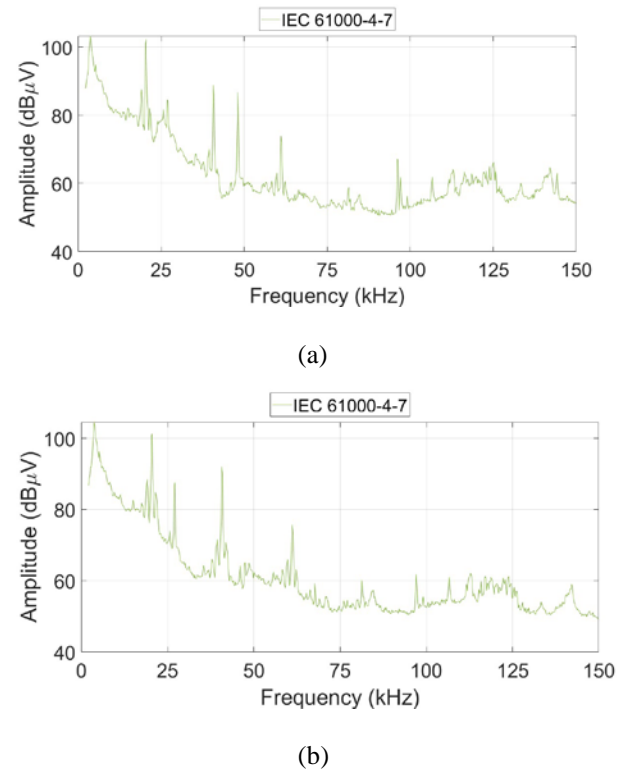


Fig.12. NIEs at grid connected installation processed using the IEC 61000-4-7 method; (a) with the inverter switched on, (b) with the inverter switched off.

4. Conclusion

This work aims to understand better the NIEs generated by PV installations. Several measurements were carried out on two isolated installations and a grid-connected system. Emissions were characterized using the CISPR 16 and the IEC 61000-4-7 method. It was observed that the NIE levels were similar for the two isolated systems, except for the highest frequencies, where the installation with the panels in parallel had slightly higher emission levels. Emissions at two different frequencies were detected due to the grid-connected system. Moreover, the significance of also making impedance measurements has been shown since, in some situations, the decrease in the impedance value when connecting a device results in the attenuation of emissions. This analysis is helpful in designing future communication protocols robust to these emissions.

Acknowledgement

This work was funded in part by the Basque Government under the grants IT1436-22, PRE_2023_2_0037 and PRE_2023_2_0162. This work was supported in part through grant PID2021-124706OB-I00 funded by MCIN/AEI/10.13039/501100011033 and by ERDF A way of making Europe.

References

- [1] Fernandez *et al.*, "Characterization of non-intentional emissions from distributed energy resources up to 500 kHz: A case study in Spain," *International Journal of Electrical Power & Energy Systems*, vol. 105, pp. 549-563, 2019.
- [2] G. F. Bartak and A. Abart, "EMI of emissions in the frequency range 2 kHz—150 kHz," in *22nd International Conference and Exhibition on Electricity Distribution (CIRED 2013)*, Jun. 2013, pp. 1-4.
- [3] European Committee for Electrotechnical Standardization-CLC/TR 50627, "Study report on electromagnetic interference between electrical equipment/systems in the frequency range below 150 kHz," 2015. [Online]. Available: <https://www.normsplash.com/Samples/BSI/172479923/PD-CLC-TR-50627-2015-en.pdf>
- [4] J. Meyer, S. Haehle, and P. Schegner, "Impact of higher frequency emission above 2 kHz on electronic mass-market equipment," in *Proceedings of the 22nd International Conference and Exhibition on Electricity Distribution (CIRED 2013)*, Jun. 2013, doi: 10.1049/cp.2013.1027.
- [5] V. Khokhlov, J. Meyer, P. Schegner, D. Agudelo-Martínez, and A. Pavas, "Immunity assessment of household appliances in the frequency range from 2 to 150 kHz," in *25th International Conference on Electricity Distribution (CIRED)*, Jun. 2019, p. 763.
- [6] N. Uribe-Pérez, I. Angulo, L. Hernández-Callejo, T. Arzuaga, D. De la Vega, and A. Arrinda, "Study of unwanted emissions in the CENELEC-A band generated by distributed energy resources and their influence over narrow band power line communications," *Energies*, vol. 9, no. 12, p. 1007, 2016.
- [7] European Commission, "Electromagnetic Compatibility (EMC) directive," 2014. [Online]. Available: http://single-market-economy.ec.europa.eu/sectors/electrical-and-electronic-engineering-industries-eei/electromagnetic-compatibility-emc-directive_en
- [8] D. Darmawardana *et al.*, "Investigation of high frequency emissions (supraharmonics) from small, grid-tied, photovoltaic inverters of different topologies," in *2018 18th International Conference on Harmonics and Quality of Power (ICHQP)*, pp. 1-6, 2018.
- [9] M. Klatt, J. Meyer, P. Schegner, and C. Lakenbrink, "Characterization of supraharmonic emission caused by small photovoltaic inverters," in *Mediterranean Conference on Power Generation, Transmission, Distribution and Energy Conversion (MedPower 2016)*, Nov. 2016, pp. 1-6.
- [10] S. Rönnerberg, M. Bollen, and A. Larsson, "Emission from small scale PV-installations on the low voltage grid," in *The Renewable Energies and Power Quality Journal (RE&PQJ)*, vol. 12, no. 5, 2014, doi: 10.24084/repqj12.427.
- [11] I. Fernandez, M. Alberro, J. Montalban, A. Arrinda, I. Angulo, and D. de la Vega, "A new voltage probe with improved performance at the 10 kHz—500 kHz frequency range for field measurements in LV networks," *Measurement*, vol. 145, pp. 519-524, 2019.
- [12] *Specification for Radio Disturbance and Immunity Measuring Apparatus and Methods—Part 1-1: Radio Disturbance and Immunity Measuring Apparatus—Measuring Apparatus*, Acronym CISPR 16-1-1, 2019.
- [13] *Electromagnetic Compatibility (EMC) —Part 4-7: Testing and Measurement Techniques —General Guide on Harmonics and Interharmonics Measurements and Instrumentation, for Power Supply Systems and Equipment Connected Thereto*, IEC 61000-4-7, 2009.
- [14] I. Fernandez, A. Arrinda, I. Angulo, D. De La Vega, N. Uribe-Pérez, and A. Llano, "Field trials for the empirical characterization of the low voltage grid access impedance from 35 kHz to 500 kHz," *IEEE Access*, vol. 7, pp. 85786-85795, 2019.